

Staggered cell-intrinsic timing of *ath5* expression underlies the wave of ganglion cell neurogenesis in the zebrafish retina

Jeremy N. Kay^{1,*}, Brian A. Link² and Herwig Baier¹

¹Department of Physiology and Programs in Neuroscience, Genetics, and Developmental Biology, University of California, 1550 Fourth Street, San Francisco, CA 94158, USA

²Department of Cell Biology, Neurobiology, and Anatomy, Medical College of Wisconsin, 8701 Watertown Plank Road, Milwaukee, WI 53226-0509, USA

*Author for correspondence (e-mail: jnk@phy.ucsf.edu)

Accepted 22 March 2005

Development 132, 2573–2585

Published by The Company of Biologists 2005

doi:10.1242/dev.01831

Summary

In the developing nervous system, progenitor cells must decide when to withdraw from the cell cycle and commence differentiation. There is considerable debate whether cell-extrinsic or cell-intrinsic factors are most important for triggering this switch. In the vertebrate retina, initiation of neurogenesis has recently been explained by a ‘sequential-induction’ model – signals from newly differentiated neurons are thought to trigger neurogenesis in adjacent progenitors, creating a wave of neurogenesis that spreads across the retina in a stereotypical manner. We show here, however, that the wave of neurogenesis in the zebrafish retina can emerge through the independent action of progenitor cells – progenitors in different parts of the

retina appear pre-specified to initiate neurogenesis at different times. We provide evidence that midline Sonic hedgehog signals, acting before the onset of neurogenesis, are part of the mechanism that sets the neurogenic timer in these cells. Our results highlight the importance of intrinsic factors for triggering neurogenesis, but they also suggest that early signals can modulate these intrinsic factors to influence the timing of neurogenesis many cell cycles later, thereby potentially coordinating axial patterning with control of neuron number and cell fate.

Key words: Zebrafish, *ath5* (*atoh7*), Proneural genes, Atonal, Sonic Hedgehog

Introduction

The vertebrate central nervous system (CNS) arises during development from specialized neuroepithelial progenitor cells, or neuroblasts. These cells first proliferate to generate the appropriate number of progenitors for each CNS region. Over time, neuroblasts eventually stop dividing and start the process of neurogenesis: that is, the series of developmental programs that causes the cell to exit the cell cycle and differentiate by assuming the phenotype of a mature neuron (Edlund and Jessell, 1999). We will refer to the switch from proliferation to differentiation as the start of neurogenesis, and to the molecular mechanism as ‘activation of the neurogenic program’. The time at which a given neuroblast activates neurogenesis is carefully regulated, as premature or tardy cell cycle exit can lead to pathological over- or underproduction of neurons (Chenn and Walsh, 2002; Zechner et al., 2003). Moreover, the relative timing of neurogenesis may be a key determinant of cell fate in many regions of the CNS (Edlund and Jessell, 1999; Livesey and Cepko, 2001). Despite the functional importance of neurogenic timing, little is known about how it is specified. Both cell-extrinsic and cell-intrinsic mechanisms have been implicated, but their relative importance is not known (Durand and Raff, 2000; Perron and Harris, 2000; Zechner et al., 2003; Edlund and Jessell, 1999).

In the retina, neurogenesis spreads through the field of

progenitors following a precise spatiotemporal pattern, the essential features of which are conserved across vertebrates (reviewed by Vetter and Brown, 2001). Retinal ganglion cells (RGCs), the first cell type to differentiate in the vertebrate retina, initially form a small patch adjacent to the site where the optic stalk attaches to the optic cup. Differentiation then progresses in a manner that, while varying somewhat between species, generally fills first the central retina and then the more peripheral retina in an orderly fashion that resembles an advancing wave front. This feature of retinal differentiation allows the timing of neurogenesis to be predicted from retinal location, an important experimental advantage. In this study we use the zebrafish retina as a model to understand how neuroblasts time their decision to become neurogenically active.

Expression of the proneural gene *atoh5* (*ath5*; *atoh7* – Zebrafish Information Network) is closely associated with the activation of retinal neurogenesis in all vertebrates. The gene encodes a basic helix-loop-helix transcription factor expressed in a wave-like pattern that prefigures the wave of RGC genesis (Masai et al., 2000). Retinoblasts that express *ath5* during this wave do so just after their final mitosis; immediately thereafter they begin to differentiate as RGCs (Yang et al., 2003). In the absence of functional *Ath5*, these cells either ectopically re-enter the cell cycle or fail to exit the

cell cycle (Kay et al., 2001), causing both a failure of RGC genesis and an overall delay in the formation of the first retinal neurons (Brown et al., 2001; Kay et al., 2001; Wang et al., 2001). These findings indicate a requirement for *ath5* in activating neurogenesis.

As yet, little is known about the control of *ath5* expression. A signal from the optic stalk, presumably FGF (Martinez-Morales et al., 2005), appears to induce the first patch of *ath5*-expressing cells (Masai et al., 2000) (but see Stenkamp and Frey, 2003). How *ath5* spreads from that initial patch to cover the rest of the retina is not known, but there is a dominant hypothesis predicting the cellular and molecular mechanisms controlling this process (Amato et al., 2004; Hsiung and Moses, 2002; Jarman, 2000; Kumar, 2001; Malicki, 2004; Neumann, 2001). The hypothesis originated with the observation that vertebrate retinal neurogenesis is reminiscent of the wave-like progression of neurogenesis across the *Drosophila* eye field. In the fly, the *ath5* ortholog *atonal* (*ato*) is expressed in a stripe just ahead of the morphogenetic furrow, which contains the differentiating photoreceptors. Both the *ato* stripe and the furrow advance across the eye imaginal disc due to Hedgehog (Hh) secretion by newborn photoreceptors (reviewed by Kumar, 2001). Hh triggers expression of *ato* in progenitor cells ahead of the furrow; *Ato* in turn causes formation of the next group of photoreceptors, which secrete their own Hh, thus forming a self-propagating wave that spreads by sequential induction of new neurons. Loss of *ato* function blocks photoreceptor formation, thereby removing the cellular source of Hh and bringing the wave to a halt (Jarman et al., 1995).

By analogy with the mechanism in *Drosophila*, it has been hypothesized that signals derived from newborn RGCs, particularly Sonic hedgehog (Shh), might drive the *ath5* wave. In support of this idea, *shh* is expressed by newborn RGCs, and *shh* expression spreads across the zebrafish retina in what appears to be a self-propagating wave (Zhang and Yang, 2001; Neumann and Nüsslein-Volhard, 2000). Together, these findings have led to a model predicting that Hh molecules, released by RGCs, should drive progression of the *ath5* wave and hence the wave of RGC differentiation. We call this, in short, the 'sequential-induction' model.

The central prediction of this model, that continuing production of RGCs should require the presence of earlier-born RGCs, has been tested using explant cultures, but results have been conflicting (Masai et al., 2000; McCabe et al., 1999). Here, we devised in-vivo tests of the sequential-induction model, using embryological manipulations and mutant analysis in zebrafish. Our findings reveal that cell-intrinsic factors are sufficient to activate neurogenesis in the zebrafish retina, but also that cell-cell signals may act earlier in development to establish these cell-intrinsic factors or to modulate their activity in order to bring about retinotopic differences in the timing of neurogenesis.

Materials and methods

Zebrafish strains and maintenance

We used wild-type zebrafish of the TL strain. The following mutant and transgenic strains were used: *lak*^{th241}; *syu*⁴ (Tübingen Stock Center); *Tg(Pax6DF4:mGFP)*^{s220} (Kay et al., 2004); *ath5:GFP* (Masai et al., 2003); *Tg(Brn3c:mGFP)*^{s273t} (Xiao et al., 2005); *Tg(H2AF/Z:GFP)*^{kca66} (Pauls et al., 2001).

In order to accurately assay wave progression, we developed a protocol that ensured developmental synchrony across individuals. Embryos were raised at low density (no more than 50 embryos/100 mm Petri dish or 20 embryos/35 mm dish) at 27°C. All times post-fertilization reported here (aside from those cited in other works) refer to time at 27°C. For some experiments, *ath5:GFP* carriers were raised at 24°C from 12 hours post-fertilization (hpf). These embryos were staged either by counting somites or by adjusting to hpf at 27°C based on the extent of *ath5* wave progression. As a result of raising the embryos at 27°C (rather than 28.5°C), the onset and progression of the *ath5* wave in our experiments was slightly later than previously reported (Masai et al., 2000; Masai et al., 2005). In control experiments (not shown), we reared embryos at 28.5°C and found that the timing of the wave was identical to that previously reported.

Histology

Embryos were treated with phenylthiourea (PTU; 0.2 mM) to inhibit pigmentation and fixed in 4% paraformaldehyde/1× PBS overnight at 4°C. Whole-mount immunostains were performed as described (Kay et al., 2001) using the following primary antibodies: Mouse zn5, zn8 and zpr1 (Oregon monoclonal bank); mouse anti-Hu (Molecular Probes); rabbit anti-GFP (Molecular Probes). Secondary antibodies made in goat (Molecular Probes) were conjugated to Alexa488, Alexa546 and Alexa405. Images were collected using a BioRad confocal microscope and were processed with Image J and Adobe Photoshop.

An *ath5* antisense DIG-labeled RNA probe of ~700 bp was made for in-situ hybridization by cloning the *ath5* cDNA (Kay et al., 2001) into pCS2, cutting with *Bam*HI, and transcribing with T7 polymerase. This probe also detected the *ath5:GFP* transgene mRNA due to the inclusion of the *ath5* 3' UTR in the transgene construct. To identify *lak* mutants, *ath5* staining was followed by either RFLP mapping (Kay et al., 2001) or by immunofluorescent labeling with the anti-Hu antibody (not shown). Templates for synthesizing *patched1* and *patched2* riboprobes were a gift of J. Eisen (Oregon). Brightfield images were collected using a CCD camera (Spot).

Generation of *lak*/wild-type chimeras

Embryos from a *lak*/+ incross were used to generate chimeras by transplantation of blastula cells at the 1000-cell stage, as described (Ho and Kane, 1990; Kay et al., 2004). At 55 hpf, hosts were fixed and stained with zn5 antibody and streptavidin:Alexa 546 (Molecular Probes) to reveal donor cells. Donors were genotyped at the *lak* locus by RFLP (Kay et al., 2001). The absence of zn5 expression identified *lak* mutant hosts.

Retinoblast transplants

Retina-to-retina transplants

Donor embryos hemizygous for *ath5:GFP* were labeled by injection at the 1-4 cell stage with rhodamine- and biotin-dextran amine (RDA/BDA) in 120 mM KCl (5% w/v). Host embryos (also *ath5:GFP*/+) were uninjected siblings. Cells were removed from the donor retina using a glass micropipette attached to a microsyringe drive (Stoelting Co.). Transplants were begun when the hosts were ~24 hpf and continued until ~26 hpf. In order to ensure that GFP⁺ cells were not transplanted accidentally, cells were never taken from the ventronasal patch itself, but rather from more dorsal regions of nasal retina. We confirmed by in-situ hybridization that the *ath5:GFP* transgene was not expressed there at this age (not shown). Grafted cells did not begin expressing GFP for several hours, further suggesting (as GFP folds and becomes fluorescent quickly) that GFP mRNA was not present at the time of transplant. After transplantation, embryos were examined periodically for GFP expression until 58 hpf, using a Zeiss Axioskop II microscope and a 20× air or 40× water-immersion lens. Further images were collected from live fish using the BioRad confocal microscope. Depending on the exact location into which the donor cells settled, the difference between the predicted

differentiation time of the original location of the donor cells and their new location could be quite small. In order to increase this time window, and thereby make more of the transplants informative, we delayed development of the hosts by maintaining them at 24°C starting at 12 hpf. This delayed start of the host wave relative to donors by ~5 hours.

Retina-to-brain transplants

RDA/BDA-labeled *ath5:GFP* hemizygous embryos were used as donors; age-matched TL (wild-type) embryos were used as hosts. Retinoblasts were removed (as described above) from the central or temporal retina and placed into the head mesenchyme or brain ventricles of a host. Immediately after transplant, and at various times thereafter until 58 hpf, the live hosts were examined for the presence of GFP expression. Importantly, no grafts expressed GFP at the time of transplantation. Donors ranged in age from 20 somites to 29 hpf, depending on the experiment.

RT-PCR methods

Embryos at the 22–24-somite stage, or 35 hpf as a positive control for *ath5* expression, were homogenized in Trizol reagent (Gibco). Total RNA was isolated according to the manufacturer's instructions. Two separate RNA samples were prepared for each time point, yielding identical results. First-strand cDNA for *ath5* or *cdc16* (a ubiquitously expressed positive control) (A. M. Wehman and H.B., unpublished) was synthesized (Promega reverse transcriptase) using the gene-specific primers 5'-TTTCGTAGTGGTAGGAGAAAG for *ath5* and 5'-TCCAACACAGAGGACACGAT for *cdc16*. A 300 bp *ath5* PCR product was generated using the 'RFLP' primers described (Kay et al., 2001). A ~200 bp *cdc16* PCR product resulted using the primers 5'-CATGGTTTGCTGTTGGATGT (forward) and 5'-GGCCTGGT-CATGTTCACTCT (reverse).

Laser ablation

The ablation method and equipment are described by Roeser and Baier (Roeser and Baier, 2003). In one set of experiments, animals were at the 22–28 somite stage; in another set they were at 24–26 hpf. A single *Pax6DF4:mGFP* embryo was transferred to the agarose-coated lid of a 35 mm Petri dish. The weight of the embryo caused it to lie on its side, eye up. The liquid level (embryo medium + 0.02% Tricaine as anesthetic) was adjusted so that the embryo was barely submerged. The ventronasal region of one eye was irradiated with the laser until GFP fluorescence in the targeted area was thoroughly quenched (~1–2 minutes/embryo). Following staining for *ath5*, we verified that ablations had indeed killed the ventronasal cells by locating pyknotic cells using DIC optics.

Drug treatment

Dechorionated TL embryos were treated with cyclopamine or vehicle (DMSO or methanol), fixed and stained with *ath5*, *ptc1* or *ptc2* riboprobes. Cyclopamine was obtained from Toronto Research Chemicals and by the generous gift of Dr J. K. Chen (Johns Hopkins/Stanford). We tested dosages between 100–400 µM, but for all experiments shown and quantified here we used cyclopamine at 200 µM, which has been shown by real-time RT-PCR analysis to be optimal for blocking all Hh dependent transcription (Wolff et al., 2003).

Quantification of wave position in *syu* and cyclopamine experiments

The position of the *ath5* or RGC wave front was determined by examining stained embryos (labeled with either the *ath5* riboprobe or with *zn5*/anti-GFP antibodies) on a Leica MZ-FLIII dissecting microscope or the Zeiss compound microscope using 10× or 20× objectives. Each animal was scored as belonging to one of four categories: (1) wave front in ventronasal retina; (2) wave front in central retina; (3) wave front in temporal retina; or (4) wave over (*ath5*

expression only in the ciliary margin or RGCs evenly filling the GCL). Because vehicle-treated animals from cyclopamine experiments (both 13 and 25 hpf groups) were indistinguishable from untreated wild-type *syu* siblings, we pooled the data from these groups into a single 'wild-type' category.

Results

The *ath5* wave progresses in the absence of RGCs

The wave of *ath5* expression and RGC differentiation in zebrafish occurs during the second day post-fertilization, with *ath5* leading RGC differentiation by several hours (Hu and Easter, 1999; Masai et al., 2000). In order to formulate a sensitive assay for progression of the neurogenic wave, we developed a protocol for synchronizing development of zebrafish larvae such that all the wild-type embryos at a given time point showed essentially identical *ath5* expression patterns when stained by in-situ hybridization. Staining up to 50 embryos at a time, the position of the *ath5* wave front varied by only a few cell diameters across individuals in a given experiment (not shown), and was also very consistent across experiments (see below). Our protocol included lowering the temperature to 27°C to slow down development (see Materials and methods). Under these conditions, *ath5* expression commenced in the ventronasal patch consistently at 30 hours post-fertilization (hpf). When the fish were raised at 28.5°C, *ath5* was first detectable by in-situ hybridization at 25 hpf, as reported previously (Masai et al., 2000). Unless otherwise noted, all fish ages given here were measured at 27°C.

Fig. 1 shows both the *ath5* and RGC differentiation waves, revealed either by staining for *ath5* mRNA (Fig. 1A–C); staining for the *zn5* antigen (Trevarrow et al., 1990), a specific RGC marker (Fig. 1G–L); or by expression of an *ath5:GFP* transgene (Masai et al., 2003) that faithfully recapitulates the spread of *ath5* mRNA across the retina (Fig. 1D–F; compare with Fig. 1A–C). The *ath5* wave starts in the ventronasal retina (Fig. 1A,D) with an initial cluster of cells known as the ventronasal patch (Hu and Easter, 1999), and spreads from there to fill the rest of the nasal retina and then a small patch of the central retina (Fig. 1B,E). Next the wave begins spreading in a central-to-peripheral manner, filling increasingly more peripheral regions of dorsal and temporal retina. Ventrotemporal retina is the last to express *ath5* and to make RGCs (Fig. 1C,F) (Hu and Easter, 1999).

The sequential-induction model predicts that spread of the *ath5* wave should require RGC-derived signals. To test this hypothesis, we used the zebrafish *lakritz* (*lak*) mutant, in which a null mutation in the *ath5* gene causes complete elimination of RGCs (Kay et al., 2001). We found that the spread of *ath5* expression was normal in *lak* mutants (Fig. 2 and data not shown; *n*>10 mutants and >20 wild-type siblings for each time point). Thus, neither RGCs nor the *ath5* gene itself are essential for driving the *ath5* wave.

RGCs form without sequential induction by pre-existing RGCs

We next tested whether signals from earlier-born RGCs are essential for driving the RGC differentiation wave. Because the *lak/ath5* gene acts cell-autonomously in RGC specification (Fig. 3D–H), we were able to test this prediction by generating *lak*/wild-type chimeras in which a small number of wild-type

cells were situated in an otherwise mutant (and thus RGC-free) retina (see model, Fig. 3C). We generated chimeras at the 1000-cell stage (Ho and Kane, 1990) and assayed RGC differentiation at 55 hpf using the *zn5* antibody. Regardless of the host's genotype, retinal clones derived from *lak* mutant donors never gave rise to *zn5*⁺ RGCs ($n > 50$ clones; Fig. 3G,H), while clones from wild-type donors always did. Of the wild-type-into-*lak* chimeras ($n = 9$ eyes with multiple clones per eye), we found three retinæ with central or temporal clones that were well isolated from both the optic stalk and other RGC-containing wild-type clones. Contrary to the sequential-induction model's predictions, the isolated clones gave rise to RGCs in all three cases (Fig. 3E,F and data not shown). Indeed, clones in the temporal retina could produce RGCs even when the rest of the retina was completely devoid of RGCs (Fig. 3F). Thus, RGC formation in later-differentiating retinal regions does not depend on prior RGC formation in earlier-differentiating regions.

Laser ablation of the ventronasal patch does not block the *ath5* wave

We next asked whether the *ath5*-expressing retinoblasts themselves might signal to neighboring retinoblasts, inducing them to express *ath5* (Masai et al., 2000). If this version of the

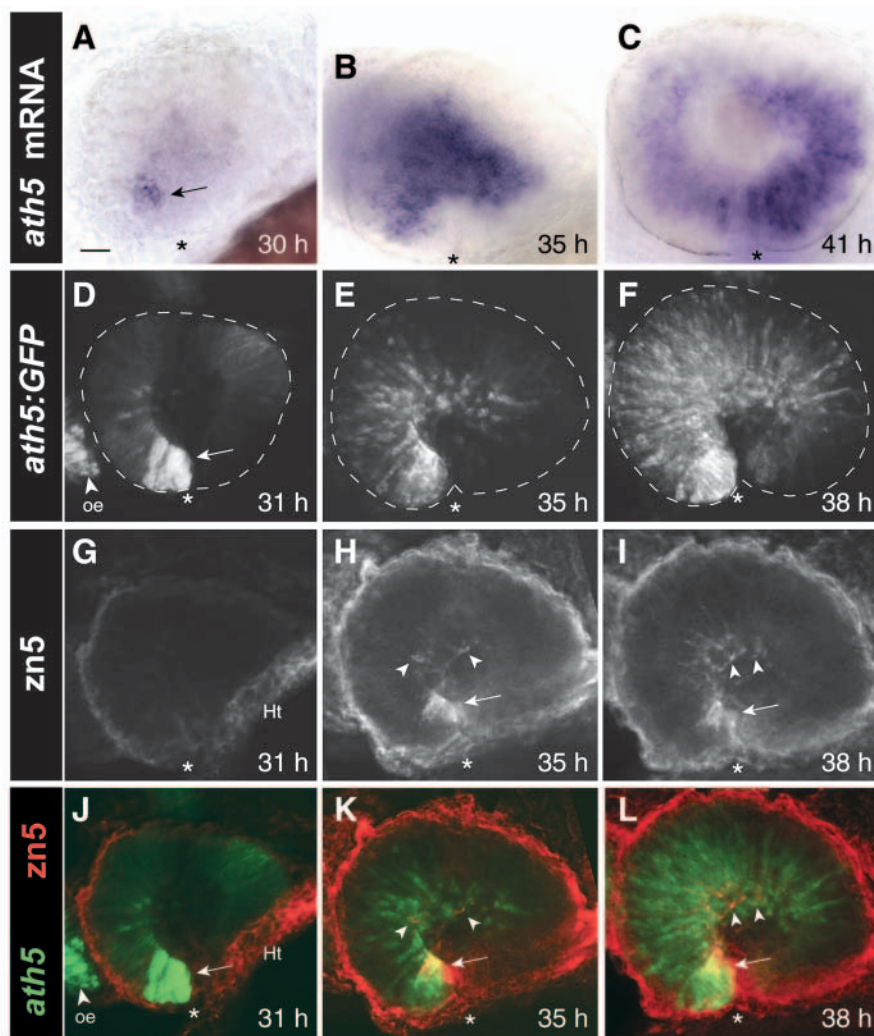
sequential-induction model is correct, then removal of the ventronasal patch before *ath5* expression should prevent relay of *ath5*-inducing signals, thereby blocking the wave. To test this prediction, we laser-ablated the neuroblasts of ventronasal retina at times ranging from 22 somites to 26 hpf. To guide the ablations we used a transgenic line that expresses GFP in all retinal neuroblasts (*Pax6-DF4:mGFP^{s220}*) (Kay et al., 2004). Photobleaching of GFP protein allowed us to precisely delineate the retinal region targeted in each larva (Fig. 4A-B).

We first tested whether the laser could efficiently kill cells in the targeted ventronasal region and prevent initiation of *ath5* expression. Only one eye was treated; the other served as an internal control. Fixing and staining for *ath5* at 30 hpf, when expression is normally confined to the ventronasal patch, we found that all of the intact eyes showed the expected pattern, whereas none of the ablated eyes showed any *ath5* expression (Fig. 4E-F; $n = 5$ for 24-26 hpf ablations and $n = 6$ for 22-somite ablations). Most of the tissue in the laser-targeted region was dying or dead, as evidenced by the pyknotic morphology of the cells (Fig. 4C-D) (Li et al., 2000). To ensure that the ablations eliminated cells before the onset of *ath5* expression, a control group of age-matched siblings was sacrificed immediately after the ablations. None showed *ath5* expression by in-situ hybridization ($n > 30$) or by RT-PCR (age-matched progeny of a different cross; not shown). We conclude that the laser treatment was sufficient to kill most or all of the ventronasal retinoblasts, thereby preventing the normal onset of *ath5* expression and formation of the ventronasal patch.

We next tested whether elimination of the ventronasal patch would affect spread of *ath5* expression through the rest of the retina. Ablations were performed as before, but this time we assayed for *ath5* mRNA expression at 33 hpf. In ablated retinas, the

We next tested whether elimination of the ventronasal patch would affect spread of *ath5* expression through the rest of the retina. Ablations were performed as before, but this time we assayed for *ath5* mRNA expression at 33 hpf. In ablated retinas, the

Fig. 1. The spatiotemporal pattern of RGC neurogenesis in zebrafish. Spread of *ath5* mRNA (A-C), *ath5:GFP* (D-F) and RGC differentiation (G-I) across the retina. (A-C) Whole-mount embryos stained with an antisense *ath5* riboprobe. (D-I) Whole-mount embryos double-stained with anti-GFP (D-F) and *zn5* (G-I) antibodies. (J-L) Merge of D-F (*ath5:GFP*, green) with G-I (*zn5*, red), showing that the *ath5* wave leads the RGC differentiation wave by several hours. D-L are z-projections of stacks of confocal images. Arrows in A,D and H-L indicate the ventronasal patch. No RGCs are present at 31 h (G), although *zn5*-immunoreactive tissue is seen in the heart (Ht). Arrowheads in H-I and K-L indicate *zn5*⁺ RGCs. Note that *ath5* RNA expression is transient, becoming downregulated behind the wave (C), whereas GFP expression (F) persists longer and thus acts as an indelible marker of all cells that have expressed *ath5*. Asterisks mark the location of choroid fissure, which delineates the boundary between nasal and temporal retina. Anterior (nasal) is left and dorsal up in all figures. Scale bar: 25 μ m. oe, olfactory epithelium; Ht, heart.



ventronasal portion of the *ath5* domain was absent, indicating successful removal of the ventronasal patch. However, outside the laser-targeted region, *ath5* expression was similar to that seen in unablated retinas (Fig. 4G-H; see Fig. S1 in the supplementary material). In all treated animals ($n=27$ at 24–26 hpf; $n=12$ at 22–28 somites), the extent of *ath5* wave progression into the central retina was the same in both the ablated and unablated eyes. The *ath5* wave evidently can skip over the ablated region, and begin instead in more dorsal regions of the nasal retina, in the central retina, or even in the temporal retina, depending on the size of the ablated domain (see Fig. S1 in the supplementary material). This finding indicates that, if *ath5*⁺ cells do in fact generate signals that induce *ath5* expression in neighboring retinoblasts, such signals are not necessary for propagating the *ath5* wave across the retina.

Retinal signals are not required for *ath5* expression

The results of our experiments so far suggested that cell-cell signaling is not as essential for triggering *ath5* expression as had previously been assumed. We therefore wondered whether retinoblasts would express *ath5* even when removed entirely from the normal retinal signaling milieu. To test this possibility, we devised a method for transplanting retinoblasts from a labeled donor retina into non-retinal tissues of an unlabeled host (note that this experiment is quite different from the *lak*/wild-type blastula transplants; see Materials and methods). If retinal signals are required to trigger *ath5* expression, heterotopically transplanted retinoblasts should fail to express *ath5*. Donor cells (labeled with RDA and carrying the *ath5:GFP* transgene) were removed from the temporal retina at various times between the 20-somite stage and 29 hpf. This latest time point is still ~5 hours before the first temporal retinal cell expresses mRNA for the *ath5:GFP* transgene (data not shown). Donor cells were placed in the telencephalic or mesencephalic ventricular space of a wild-type, non-transgenic host brain; some transplants were also placed in the head mesenchyme. By 50 hpf, grafted cells in both the ventricular space (Fig. 5A-B) and the head mesenchyme (not shown) expressed GFP. Some of these cells had clearly differentiated into RGC-like neurons, as they possessed long axons tipped by growth cones (Fig. 5B). To ensure that the transplants were done before the onset of *ath5* expression, we used donors at the 20–24-somite stage. RT-PCR experiments showed that *ath5* is not yet expressed at 24 somites (not shown). Three of the seven grafts from 20–24-somite donors expressed *ath5:GFP* by 50 hpf. These results demonstrate that retinoblasts can express *ath5*, and possibly even assume the RGC fate, even when stripped out of the retinal neuroepithelium and placed in a variety of ectopic locations.

We next tested whether the transplanted retinoblasts could undergo neuronal differentiation. We found that heterotopically grafted retinoblasts in the brain, brain ventricles or head mesenchyme, as well as homotopically

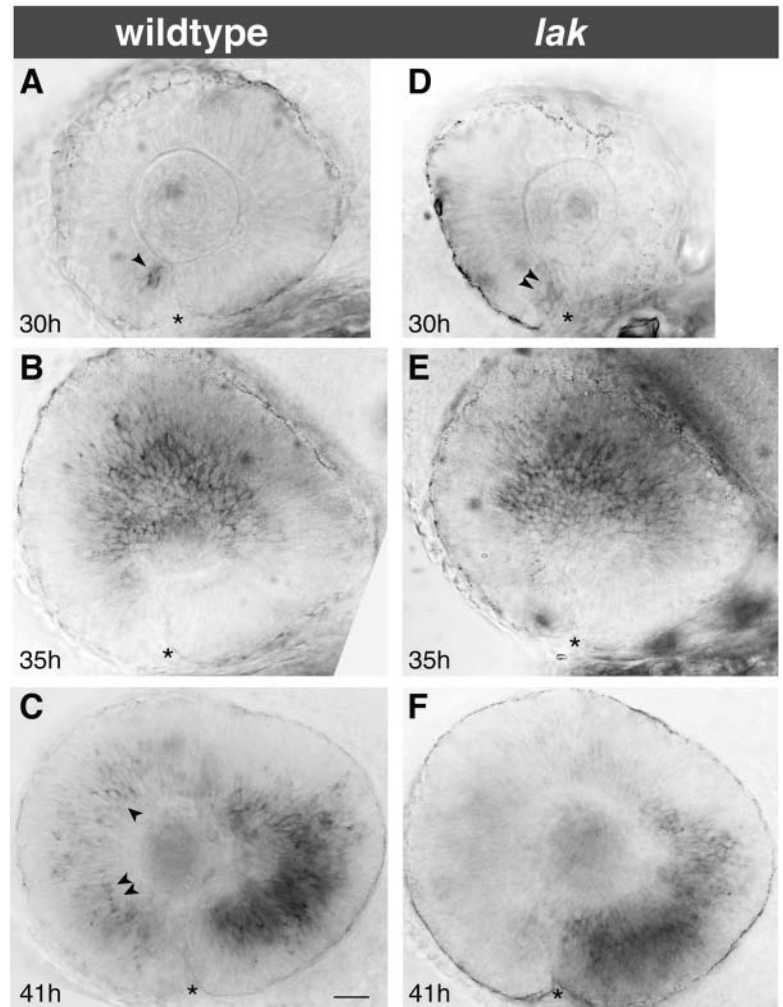


Fig. 2. RGCs are not required for spread of *ath5* expression. (A–C) Expression of *ath5* mRNA at 30 hpf (A), 35 hpf (B) and 41 hpf (C) in wild-type fish from a *lak*^{+/+} incross. At 41 hpf (C), the *ath5* wave has progressed into the ventrotemporal retina and has cleared out of the anterior and central regions, but occasionally cells behind the wave front still express *ath5* (arrowheads). (D–F) Progression of *ath5* wave in *lak* mutants is indistinguishable from wild-type. Expression of *ath5* behind the wave front is reduced in *lak* mutants, perhaps due to autoregulation of *ath5* expression (F; compare with C). Anterior (nasal) is left and dorsal up in all images. Asterisks indicate choroid fissure. Scale bar: 25 μ m.

grafted cells in the retina, could differentiate as both RGCs and photoreceptors, as judged by expression of cell-type-specific markers (see Figs S2, S3 in the supplementary material). Not every grafted cell was able to differentiate successfully. For example, only ~15–35% of cells transplanted to the host retinal ganglion cell layer (GCL) successfully expressed RGC markers by 72 hpf (see Fig. S2 in the supplementary material). This observation suggests that certain cell-cell signals, perhaps those provided by being part of an intact neuroepithelium, may be permissive for the activation of neurogenesis and/or for differentiation. Nevertheless, intra-retinal signals do not appear essential for activation or execution of the retinal neurogenic program, as both *ath5* expression and cell-type-specific marker expression can occur in the absence of such signals.

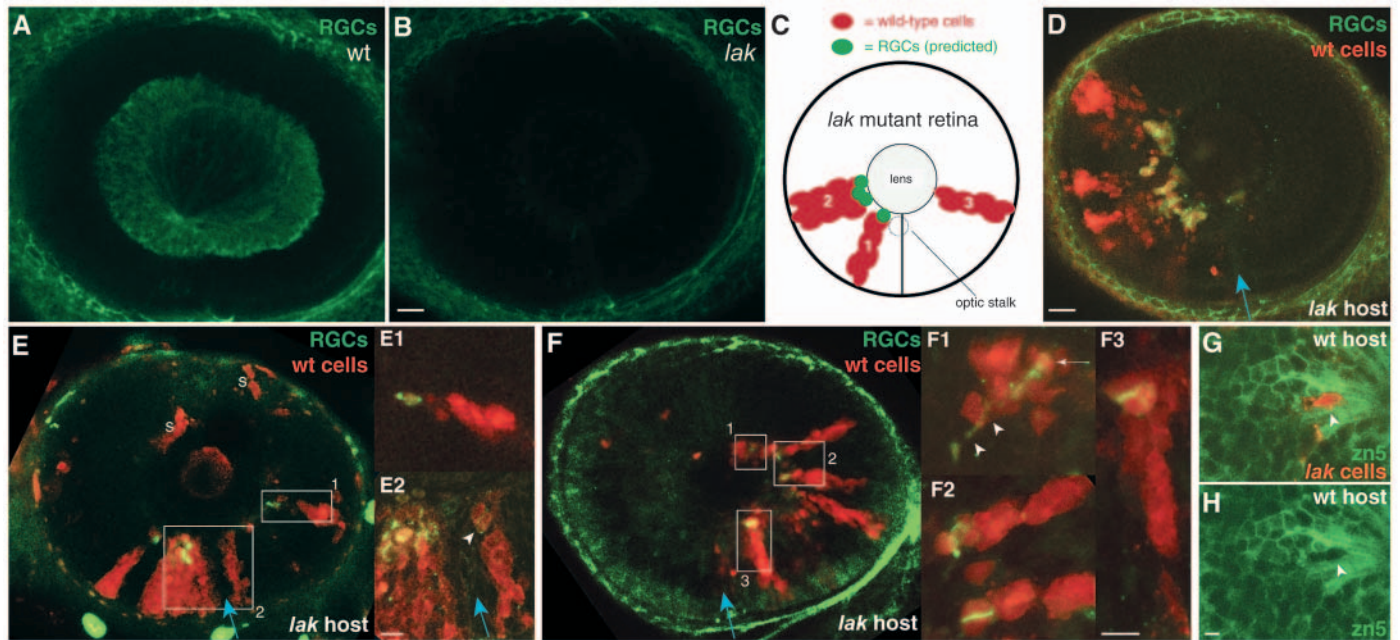


Fig. 3. RGC neurogenesis in the absence of RGC-derived signals. (A,B) Zn5 staining of wild-type (A) and *lak* mutants (B) at 55 hpf. Mutant retina is devoid of RGCs. (C) Schematic showing predicted results of transplant experiments, based on the sequential-induction model. Red cells represent wild-type clones in a *lak* mutant retina. The clone marked 1 is predicted to give rise to RGCs (green) because it is near the optic stalk (dashed circle). Clone 2 is predicted to give rise to RGCs because it is near clone 1, which contains earlier-born RGCs. Clone 3 is located far from the optic stalk and from RGCs; the model predicts it should fail to give rise to RGCs. (D-F) Wild-type-into-*lak* chimeras. (D) Only wild-type cells (red) give rise to zn5⁺ RGCs (green). (E) A wild-type-into-*lak* chimera that challenges the sequential-induction model. One clone (E1) is completely surrounded by mutant tissue and yet still forms RGCs (green). (E1, E2) High-magnification views of indicated boxed areas, showing expression of RGC markers (green) by wild-type cells (arrowhead). Both are at the same scale. (F) A wild-type-into-*lak* chimera in which donor cells are present only in temporal retina. These clones give rise to zn5⁺ RGCs. (F1-F3) High-magnification views of boxed areas (all are at the same scale). In F1, an axon (arrowheads) extends from the double-labeled RGC cell body (arrow). (G,H) A *lak*-into-wild-type chimera, showing that *ath5* is cell-autonomously required for RGC formation. Mutant donor cells (red; arrowhead) are the only cells in the GCL not labeled with zn5 (green). (H) The same field of view, showing zn5 alone to illustrate the gap in zn5 expression where the *lak* cells are (arrowhead). Anterior/nasal is left and dorsal up in all images. The blue arrow indicates the choroid fissure. S, donor-derived skin cells, not in neural retina; wt, wild type. Scale bars: in B,D, 20 μ m for A,B,D,E,F; 5 μ m for E2,F3,H.

Transplanted retinoblasts time *ath5* expression according to original location

Signaling between retinoblasts, while not necessary for *ath5* expression, might be required to produce accurate timing of the *ath5* wave. Alternatively, each retinoblast might be intrinsically programmed to activate neurogenesis on a staggered schedule, depending on its retinal position. To distinguish between these possibilities, we performed two retinoblast transplant experiments.

We first took nasal retinoblasts from RDA-labeled *ath5:GFP* carriers at 24–26 hpf and placed them into the temporal region of a host *ath5:GFP* retina. GFP expression was then monitored in live fish at regular intervals (generally ~1–2 hours), until well after the wave was complete (58 hpf). We found that these nasal-derived cells in temporal retina either began expressing *ath5* while the host wave was still confined to nasal retina (Fig. 5C,D; 31%; $n=4/13$), or failed to express *ath5* at all by 58 hpf ($n=9/13$). None of the grafted nasal cells expressed *ath5* on a temporal schedule. This result supports the notion that intrinsic factors, not signals from the advancing wave front, determine the timing of *ath5* expression. Although only 30% of nasal-into-temporal grafts succeeded in expressing *ath5:GFP* by 58 hpf, this rate of differentiation was typical for grafts into the GCL that were made without regard to the retinal sector from

which the cells were taken from or where they were placed (see Fig. S2 in the supplementary material). It is therefore unlikely that the temporal environment inhibited nasal donor cells from differentiating.

We next asked whether relative timing differences would be maintained even in the absence of retinal signals. Using RDA-labeled *ath5:GFP* carriers as donors, retinoblasts were removed from either the central or temporal retina at 26–29 hpf and transplanted into the head of wild-type (non-transgenic) hosts. This time point was several hours prior to the onset of transgene mRNA expression in the central or temporal retina (not shown). Each donor gave rise to two hosts, one carrying the donor's central retinal cells and one carrying its temporal cells. These live hosts were then checked periodically for *ath5:GFP* expression in the grafted cells. In each pair of hosts, the one carrying the central graft always expressed *ath5:GFP* first. In fact, all the central grafts had begun expressing *ath5* before the first temporal graft did so (Fig. 5B; $n=5$ central, $n=5$ temporal). Only one graft failed to express *ath5* at all ($n=11$ hosts). Thus, progenitors do not require retinal signals after 26 hpf (27°C) to maintain the neurogenic timing conferred by their original retinal position. These experiments suggest that the spatiotemporal pattern of the RGC differentiation wave might arise because retinoblasts

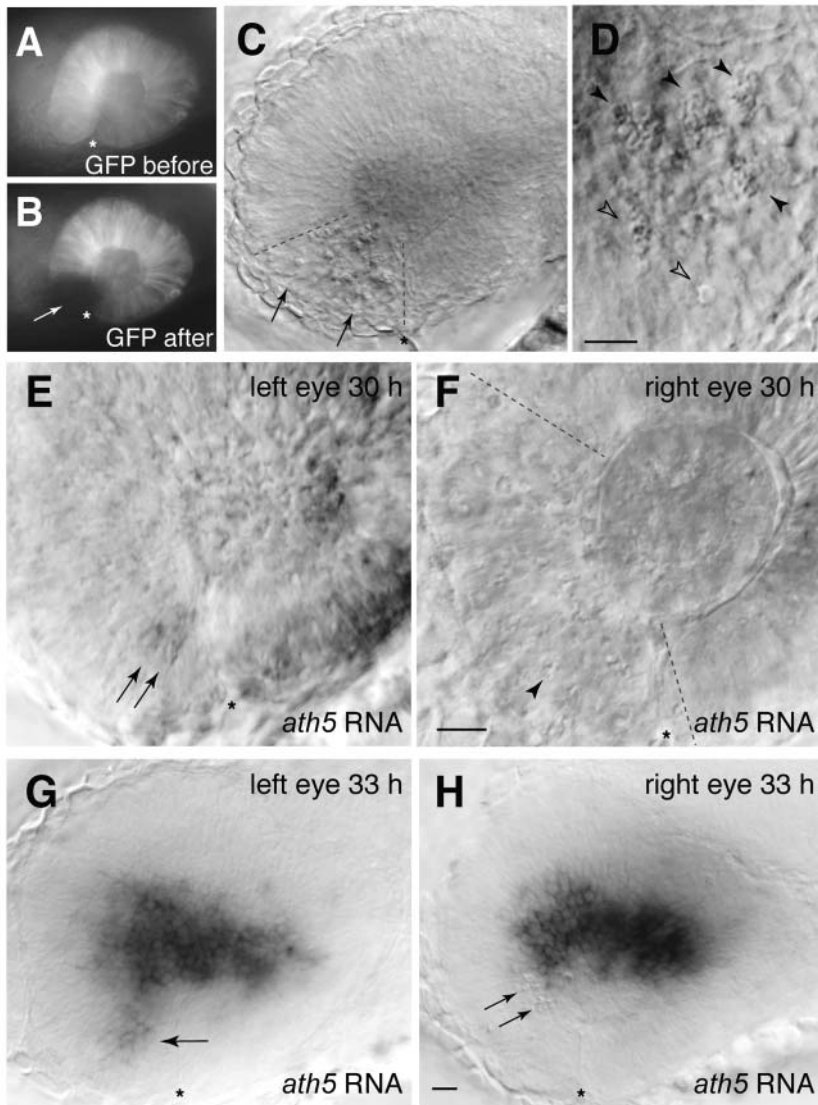


Fig. 4. Laser ablation of the ventronasal retina does not block the spread of *ath5* into the central retina. (A,B) Targeting of ventronasal retina for laser ablation. A single larva homozygous for the *Pax6DF4:mGFP^{s220}* transgene was photographed before (A) and immediately after (B) the ablation procedure. The laser-targeted region is no longer fluorescent (arrow). (C-F) Laser-targeting of ventronasal retina at 24 hpf efficiently kills cells and prevents *ath5* expression. (C) Pyknotic nuclei (arrows) were visible using DIC illumination and were found specifically within the laser-targeted region (delineated with dashed lines in C,F). Higher magnification (D) shows the characteristic pyknotic morphology of the dying cells (closed arrowheads indicate clusters of pyknotic cells; open arrowheads indicate single pyknotic cells). (E-F) Untreated (E) and treated (F) eyes of the same larva sacrificed at 30 hpf and stained for *ath5* RNA expression. The initial patch of 2-3 *ath5*⁺ cells is present in the control eye (E, arrows) but absent in the treated eye (F). The arrowhead in F indicates one example of a pyknotic cell in the laser-targeted region. (G,H) Preventing ventronasal *ath5* expression has no effect on subsequent *ath5* expression. Untreated (G) and treated (H) eyes of a single larva ablated at 24 hpf and stained for *ath5* expression at 33 hpf. In the intact eye (G), *ath5*⁺ cells are seen in ventronasal retina (arrow), as well as nasal and central regions. In the treated eye, ventronasal *ath5* expression is abolished and pyknotic nuclei are evident (arrows). Nevertheless, nasal and central retinal *ath5* expression is normal. Nasal/anterior is to the left, dorsal is up, and an asterisk marks the location of choroid fissure in all panels. See Fig. S1 in the supplementary material for more examples. Scale bars: in D, 10 μ m; in F, 25 μ m for E,F; in H, 25 μ m for C,G,H.

are intrinsically programmed, before the wave, to begin neurogenesis at different times.

Midline-derived Sonic hedgehog acts before neurogenesis to regulate the timing of *ath5* expression and RGC differentiation

The programming of neurogenic timing could be accomplished by some of the same patterning mechanisms that create anteroposterior (AP) or dorsoventral (DV) differences in gene expression across the retina (McLaughlin et al., 2003). To test this idea, we perturbed DV patterning of the diencephalon by disrupting Hh signaling. Hh-family molecules are expressed in the ventral midline of the diencephalon and have a well-established role in patterning the eye (reviewed by Amato et al., 2004). *Shh* is also expressed within the retina during RGC neurogenesis, and this retina-derived Hh has been predicted, as part of the sequential-induction model, to regulate *ath5* expression (reviewed by Amato et al., 2004; Neumann, 2001). Thus, it was important for us to separate the effects of early, midline Hh signaling from later, intra-retinal Hh signaling.

We first examined *ath5* expression in the *shh* null mutant *syu*¹⁴ (Schauerte et al., 1998). We found that the spatial pattern of the *ath5* wave was unaffected in these mutants, but the timing of wave progression was dramatically altered (Figs 6, 7). Initiation of the wave in ventronasal retina was normal at 30 hpf (Fig. 6A,E; Fig. 7A). Subsequently, the *ath5* wave spread to the central and temporal retina as in wild type, but it did so on a delayed schedule. For example, whereas the wild-type wave reached the temporal retina at 41 hpf, in *syu* mutants the *ath5* wave was confined to the central retina at 41 hpf (Fig. 6C,G; Fig. 7C). The wave did not reach the temporal retina until 50 hpf in the mutants, indicating that temporal retinoblasts were delayed in expressing *ath5* by almost 10 hours (Fig. 6D,H; Fig. 7D). Loss of *shh* function thus did not block the *ath5* wave, but it did have a substantial effect on the time of neurogenic activation.

In order to determine whether this phenotype results from loss of midline- or retina-derived Shh, we defined the time window during which *shh* is necessary for timely wave progression. To do this, we employed the drug cyclopamine, a small molecule inhibitor of the Hh receptor Smoothened (Chen

et al., 2002). Cyclopamine treatment fully inactivated the Hh signaling pathway at the dose we used (200 μ M) (see Wolff et al., 2003), as expression of the Hh target genes *patched1* and *patched2* was severely reduced or eliminated in all tissues (Fig. 8A–B and data not shown; $n=20$ for each probe). First, we specifically blocked retina-derived Hh signaling by starting cyclopamine treatment at 25 hpf, after specification of the retinal DV axis but before *ath5* expression. We saw no effect on the progression of the *ath5* wave (Fig. 7A–D; Fig. 8C,E; $n\sim 20$ treated embryos/time point). However, when we gave cyclopamine at 13 hpf, during patterning of the DV axis but before *shh* was expressed in the retina, we observed a delay in *ath5* expression similar to that seen in *syu* mutants (Fig. 8D; Fig. 7D–E; $n=9$). Together, these results suggest that early, midline-derived *shh* signaling is required to ensure the subsequent timely expression of *ath5* by retinoblasts.

To determine whether the altered timing of the *ath5* wave also changes the timing of RGC differentiation, we analyzed the expression of two different RGC markers following 13 and 25 hpf cyclopamine treatment. Indeed, we found that treatment at 13 hpf, but not 25 hpf, delays expression of RGC-specific markers (Fig. 9). Thus, while loss of Hh signaling during the *ath5* wave has no effect on *ath5* expression or RGC differentiation, blockade of early, midline-derived Hh signals causes a delay in both the *ath5* and RGC differentiation waves. This finding raises the possibility that axial patterning

mechanisms, such as midline Hh signaling, might be involved in creating spatial differences in the timing of neurogenic activation.

Discussion

In this study we have investigated how neuroblasts in the vertebrate retina activate neurogenesis – how they switch at the appropriate time from a proliferative to a neurogenic state. Because the *ath5* proneural gene is required for this switch in the earliest-differentiating retinoblasts (Kay et al., 2001; Yang et al., 2003), we looked into the cellular and molecular factors that determine the timing of *ath5* expression. We found that retinoblasts do not require signals from the retinal environment in order to correctly time *ath5* expression. We eliminated RGC-derived signals; signals derived from *ath5*-expressing cells; and finally signals from all retinal cells. In each case at least the relative timing of *ath5* expression was normal. These experiments indicate that retinoblasts may possess a cell-intrinsic program that activates neurogenesis. The intrinsic program appears to be at least partially established by the patterning activity of midline-derived Shh. Our findings may explain the origins of the wave of RGC differentiation that sweeps across the retina: Because the timing of neurogenesis is pre-specified and staggered according to retinal position, the wave may emerge through the collective timing decisions of individual neuroblasts. In this model, progressive cell-cell signaling is not required to drive the *ath5* wave, although such a mechanism may still influence retinoblast differentiation and/or cell fate selection.

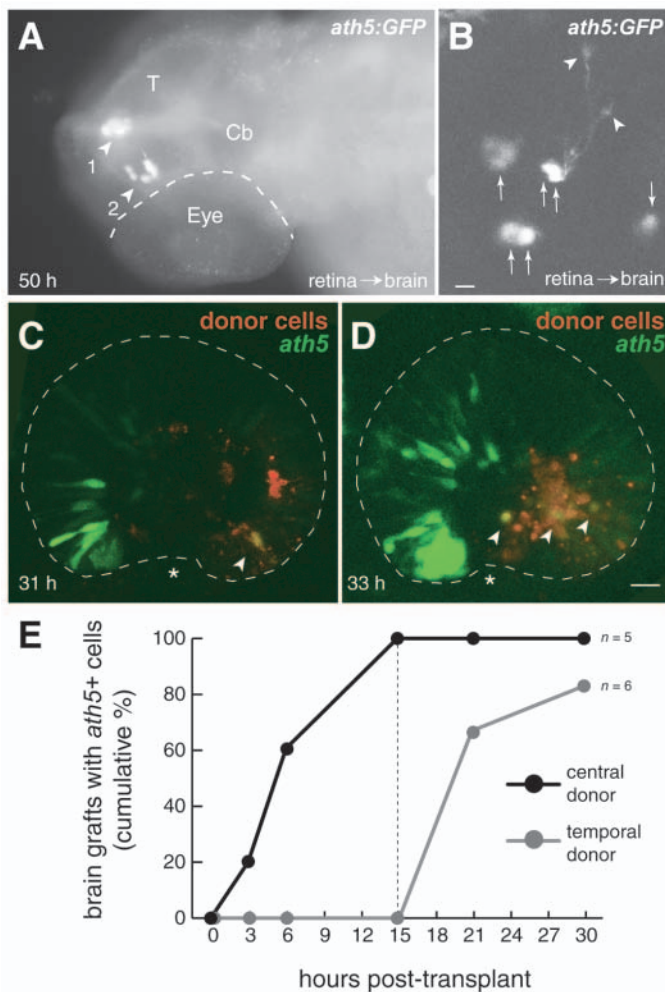


Fig. 5. Retinal position cell-autonomously specifies timing of *ath5* expression. (A,B) Retinal cells can express *ath5* and form neurons in the absence of retinal signals. (A) Cells removed from the retina (before *ath5* expression) and heterotopically transplanted into the head express *ath5:GFP* at 50 hpf. Dorsal view of fixed embryo immunostained for GFP. One cluster of GFP cells is at the dorsal midline, sitting between the epidermis and the tectum (arrowhead 1). The other GFP⁺ cluster is in the diencephalic ventricle (arrowhead 2). (B) Higher-magnification view of a different heterotopic retinoblast graft, located in the telencephalic ventricle. Single confocal scan taken from live fish at ~50 hpf. Several cells express *ath5:GFP* (arrows). Some assume a morphology typical of RGCs, with growing axons tipped by growth cones (arrowheads). Anterior is left in both panels. Ventral is down in B. (C,D) Retinal signals cannot re-specify the timing of *ath5* expression. Nasal donor retinoblasts (red) were grafted into temporal retina of an *ath5:GFP* transgenic host before onset of *ath5* expression. Subsequently, when *ath5* expression (green) had begun in host nasal retina, live hosts were imaged on a confocal microscope. Donor cells located ahead of the host's *ath5:GFP* wave front expressed GFP (yellow cells; marked with arrowheads). Each image is a z-projection of a stack of confocal images. Asterisks mark choroid fissure. Nasal/anterior is left and dorsal up in both panels. (E) The relative timing of *ath5* expression is maintained in the absence of retinal signals. Host embryos carrying either central or temporal retinal grafts in the brain ventricles were screened for *ath5:GFP* expression at various times post-transplant. The cumulative percentage of grafts expressing GFP was plotted for each time point. The central grafts (black line) expressed *ath5:GFP* before the temporal grafts (gray line). The dashed line indicates the time when all central grafts, but none of the temporal grafts, were GFP⁺. $n=11$ hosts (six temporal grafts and five central grafts). Scale bars: 5 μ m in B; 25 μ m in C,D. Cb, cerebellum; T, tectum.

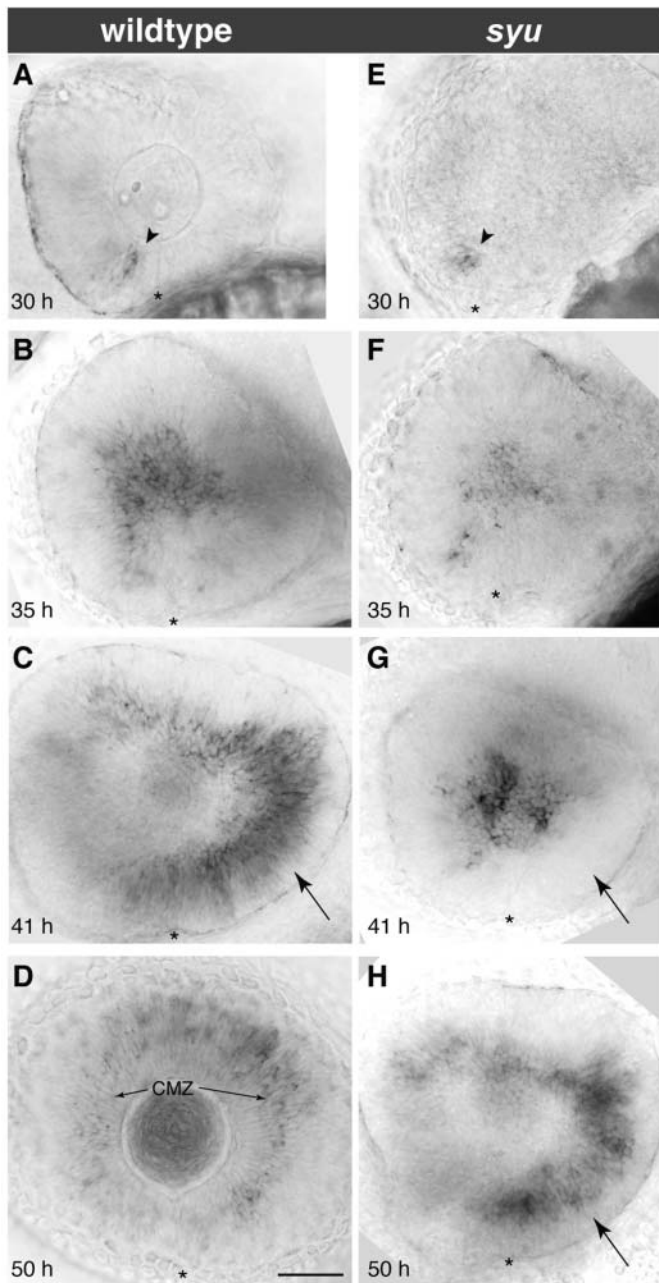


Fig. 6. Delay of the *ath5* wave caused by loss of *shh* signaling. Timecourse of *ath5* expression in wild-type or mutant embryos derived from a *syu*^{td4/+} intercross. (A–D) In wild type, the wave front is: in the ventronasal retina at 30 hpf (A); in the central retina at 35 hpf (B); and in the temporal retina at 41 hpf (C). At 50 hpf (D), the wave is over and *ath5* expression is seen only in the secondary retinal growth zone, the ciliary marginal zone (arrows in D). (E–H) In *syu* mutants, wave initiation is normal (E) but subsequently becomes delayed. About half of mutants show normal spread of *ath5* wave to central retina by 35 hpf (F); the other half fail to show expression in central retina by 35 hpf (not pictured; see Fig. 7B). By 41 hpf (G) the delay phenotype is fully penetrant – note absence of *ath5* expression in temporal retina at 41 hpf (arrow in G). By 50 hpf (H), *ath5* expression reaches the temporal retina and has cleared from the central retina, much like in wild type at 41 hpf (arrows in H,C). Nasal/anterior is left and dorsal is up in all panels. Asterisks mark the choroid fissure. Scale bar: 50 μ m. CMZ, ciliary marginal zone.

Setting the neurogenic timer: the role of midline-derived Sonic hedgehog

We show that central retinoblasts are already competent to express *ath5* independently of signals from ventronasal retina by 22 somites (~20 hpf at 28.5°C), and temporal retinoblasts are independent of retinal signals by 20 somites (~19 hpf at 28.5°C). When the retina is removed at 18 somites and the nasal and temporal halves are cultured separately, the temporal explant is delayed or fails to express *ath5* (Masai et al., 2000). This result, together with ours, may indicate that an important intra-retinal signaling event occurs between the 18- and 20-somite stages (a time window of about 1 hour). Alternatively, explanting the retina may remove a source of extra-retinal signals, such as Shh, that are required for timely differentiation of temporal retinoblasts. Regardless of the precise cellular mechanism through which the timing of *ath5* expression is set, our results are significant for showing that the time window during which signals act to influence neurogenic activation is substantially earlier than previously suspected.

If retinoblasts have an intrinsic tendency to activate neurogenesis at a particular time, there must be some mechanism that establishes the neurogenic timing for each cell. What is this mechanism, and when does it act? We find that retinal location is a key variable, implying that an asymmetric spatial signal might set the neurogenic timer in order to impart location-specific timing information. A good candidate for such a signal is Shh derived from the ventral midline of the diencephalon. Previously, midline Hh signals were reported to be required for *ath5* expression (Stenkamp and Frey, 2003). Here we extend this important finding by showing that Shh acts between 13 and 25 hpf not as an absolute prerequisite for *ath5* expression, but rather to ensure timely expression of *ath5* during the wave, hours later. Before 25 hpf, *shh* and its relative, *tiggy-winkle hedgehog* (*twhh*), are expressed in the diencephalic ventral midline but not in the retina (Ekker et al., 1995). In fact, *shh* expression is not detectable in the retina before the *ath5* wave has already reached the temporal retina (Masai et al., 2005). These combined results suggest that the midline source of Hh signals, in addition to patterning the DV axis of the eye (Amato et al., 2004; McLaughlin et al., 2003), also seems to have a role in patterning the timing of retinal neurogenesis.

In a recent study, Masai et al. (Masai et al., 2005) narrowed the time window of Hh action even further by using forskolin, a potent activator of protein kinase A (PKA), which in turn antagonizes Hh signaling. In keeping with our results, these authors show that the *ath5* wave can only be blocked when forskolin treatment occurs before, but not during, wave progression (21–25 hpf at 28.5°C) (Masai et al., 2005). Because forskolin causes a more severe *ath5* phenotype than either cyclopamine or various genetic manipulations that block Hh signal transduction, it appears that multiple signaling pathways impinge on PKA to regulate the subsequent timing of *ath5* expression.

Evidence against a role for retinal Hh signaling in *ath5* expression

Loss of early Hh signaling delays both the *ath5* and RGC differentiation waves. By contrast, retina-derived Hh appears not to be required for *ath5* expression or RGC differentiation. In *Xenopus*, chick and mouse, reducing retinal Hh signaling

has effects on RGC genesis similar to those we describe (Dakubo et al., 2003; Perron et al., 2003; Zhang and Yang, 2001). By contrast, it had previously been reported that retinal Hh signaling is essential for RGC formation in zebrafish (Neumann and Nüsslein-Volhard, 2000), a finding that we

could not confirm. It is not clear why the results of the two studies differ. In both experiments, cyclopamine was used to block Hh signaling specifically during the period of RGC genesis (starting at ~25 hpf). We show, using *ptc1/2* staining on larvae treated in parallel with those tested for RGC formation, that our drug was effective at eliminating Hh signaling. To control for drug quality, we obtained cyclopamine from two independent sources and dissolved it in two different solvents – each permutation of the experiment gave identical results.

Another line of experimentation in zebrafish recently arrived at the conclusion that short-range Hh signaling is required within the retina for progression of the *ath5* wave (Masai et al., 2005). These authors injected embryos with antisense morpholino oligonucleotides that abrogate Shh and Twhh function (Hh-MO). Cells from Hh-MO embryos were then transplanted at the blastula stage into wild-type hosts. Hh-MO cells did not express *ath5* at 33 hpf (28.5°C), the latest time point studied (equivalent to 40 hpf at 27°C), despite being surrounded by wild-type cells from the host. Host cells adjacent to Hh-MO clones also occasionally failed to form RGCs. While this finding is consistent with a role for short-range Hh signaling in the progression of the *ath5* wave, other interpretations are possible. In particular, it is unclear if analysis of donor-derived clones in the eye would allow a strict test of whether Hh signaling acts in the eyecup to regulate *ath5*. As the Hh-MO clones lack Shh/Twhh activity throughout their developmental history, the effects on *ath5* expression could reflect a requirement for Hh signaling before eye evagination. Even cell-non-autonomous effects on neighboring cells are plausible given the close juxtaposition of cells in neural plate that will later give rise to the eye (Varga et al., 1999). Furthermore, if Hh signaling propagates *ath5* expression between cells, then some of the Hh-MO donor cells near Hh-expressing host cells should have expressed *ath5*, which apparently was not seen (Masai et al., 2005). While it is possible that Hh signals act within the eye to affect *ath5* expression (perhaps by an autocrine mechanism), further

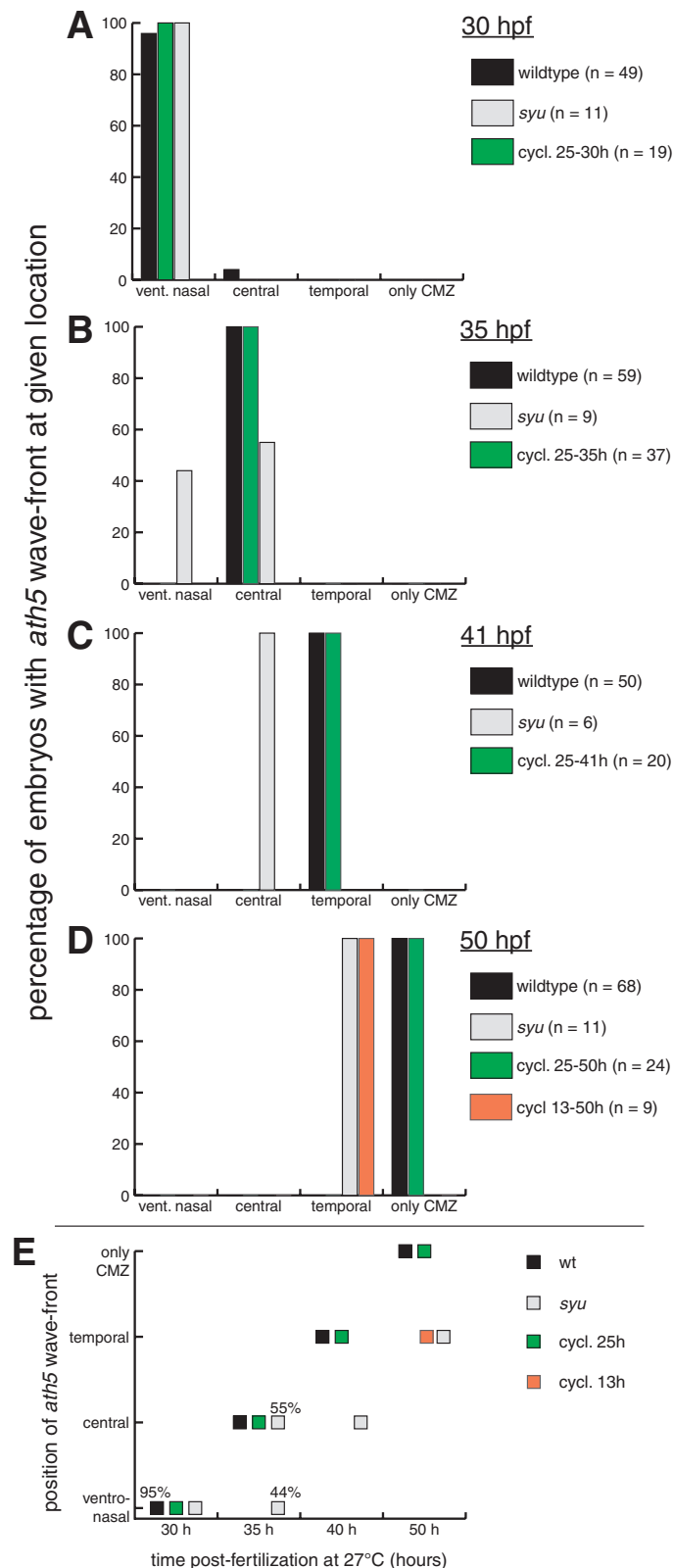
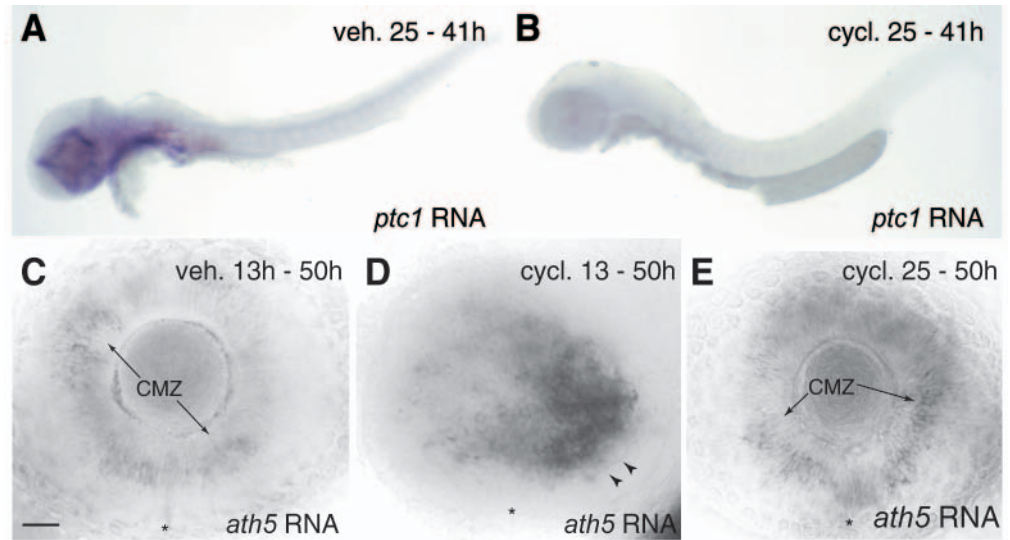


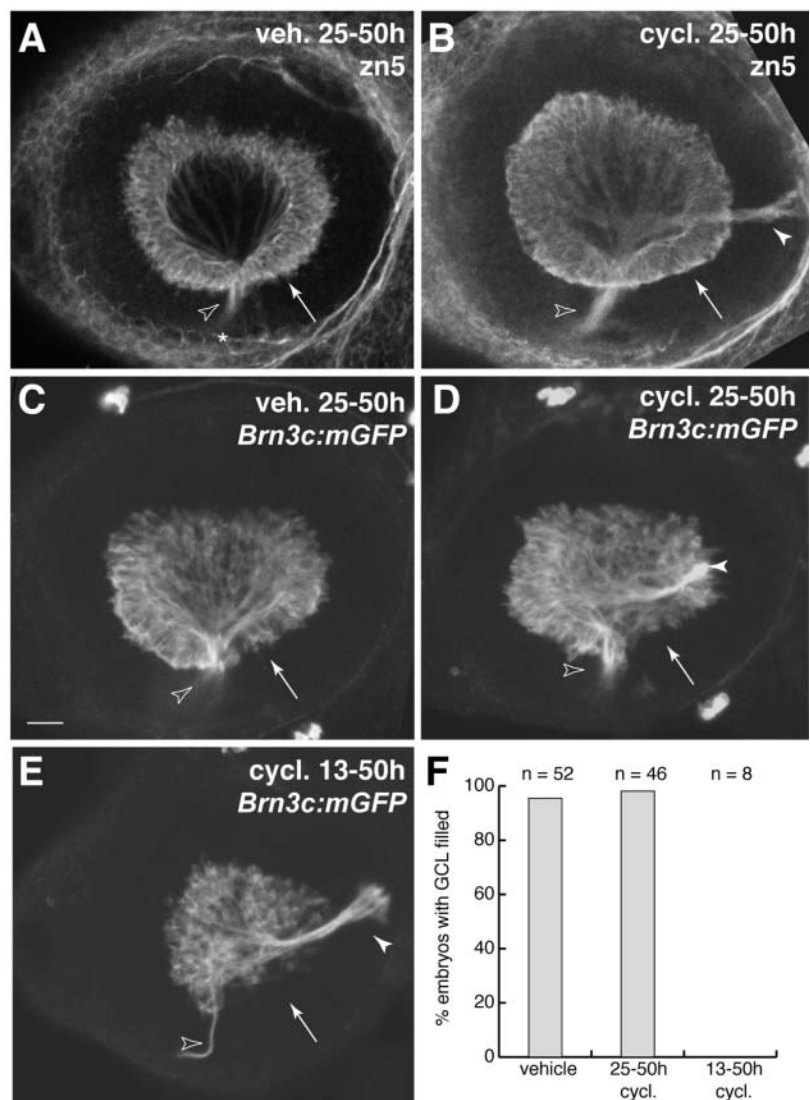
Fig. 7. Correct timing of the *ath5* wave requires Sonic hedgehog signaling before, but not during, retinal neurogenesis. (A-D) The position of the *ath5* wave front was quantified in all embryos from the *syu* and cyclopamine experiments. Each embryo was scored for the quadrant of the retina in which the wave front was located: either ventronasal, central or temporal. If the wave was over, and *ath5* expression was confined to the ciliary marginal zone the embryo was scored as 'only CMZ'. The fraction of embryos at a given age falling into each of these four categories was plotted. Because we took care to ensure developmental synchrony, in most cases, the fraction was 100%. Examples of how the *ath5* expression domain looked for each category are shown in Fig. 6A-D. (E) Summary of the results of *syu* and cyclopamine experiments. The retinal position of the *ath5* wave front as calculated in A-D was plotted for groups of wild-type, *syu* mutant and cyclopamine-treated embryos at different ages. Each data point indicates that 100% of the embryos in the given treatment group fell into the given wave-position category, unless marked by a different percentage. All values are taken from the graphs in A-D. In *syu* mutants (gray), the *ath5* wave was delayed relative to wild type (black), but it did eventually traverse the entire retina. The delay at 35 hpf showed incomplete penetrance. Starting cyclopamine treatment at 13 hpf also delayed the *ath5* wave (orange), but when cyclopamine was given at 25 hpf (green) the rate of wave progression mirrored wild type. CMZ, ciliary marginal zone; cycl., cyclopamine.

Fig. 8. Effects of cyclopamine treatment on Hedgehog pathway activity and *ath5* expression. (A,B) Expression of *patched1* (*ptc1*), a target of the Hh signaling pathway, reveals tissues in which the Hh pathway is active. Treatment from 25–41 hpf with cyclopamine (B), but not vehicle (A), drastically reduced or abolished the *ptc1* signal (blue stain), indicating effective blockade of Hh signaling. Expression of *patched2* was similarly affected (not shown). (C–E) Blockade of Hh signaling at 13 hpf, but not 25 hpf, delays the *ath5* wave. Larvae treated with cyclopamine from 13–50 hpf (D) show *ath5* expression by temporal retinoblasts (arrowheads), much like a 41 hpf wild type (Fig. 6C) or 50 hpf *syu* mutant (Fig. 6H). In vehicle-treated larvae (C), as well as larvae treated with cyclopamine from 25–50 hpf (E), the wave is over and *ath5* expression is confined to the ciliary marginal zone (arrows). Anterior/nasal is left and dorsal up in all photos. CMZ, ciliary marginal zone; cycl., cyclopamine; veh., vehicle. Scale bar: 25 μ m for C–E.



studies will be required to resolve this question definitively. Retina-derived Hh clearly has important functions in axon guidance (see Fig. 9) and in the differentiation of later-born cell types, such as bipolar cells and photoreceptors (Shkumatava et al., 2004; Stenkamp and Frey, 2003; Stenkamp et al., 2000). In any case, our studies suggest that Hh is unlikely to be required as a sequential inducer of *ath5* expression.

Fig. 9. Hedgehog signaling during retinal neurogenesis is not necessary for RGC differentiation. (A–D) Blockade of Hh signaling with cyclopamine at the start of retinal neurogenesis – 25 hpf – does not affect RGC formation. Two different RGC-specific markers, the *zn5* antigen (A–B) and a *Brn3c:mGFP* transgene (C–D) were assessed at 50 hpf. In both vehicle-treated and cyclopamine (25–50 hpf)-treated animals, RGCs filled the entire GCL, including temporal retina (arrows), by 50 hpf. Note that, in wild type (A,C), all RGC axons left the eye via the optic disc (open arrowheads), whereas in cyclopamine animals (B,D) some RGC axons formed an ectopic fascicle projecting to the posterior of the eye (closed arrowheads). (E) Treatment with cyclopamine from 13–50 hpf delays RGC genesis. Note absence of GFP-expressing RGCs from the ventral half of the temporal retina (arrow). Zn5 staining gave similar results (not shown). Axon pathfinding defects were again observed (closed arrowhead). (F) Quantification of the phenotypes shown in A–E. Data were pooled over several experiments. Nearly all the vehicle and 25–50 hpf cyclopamine animals were finished with RGC genesis by 50 hpf, as shown by even filling of the GCL with RGCs. In the 13 hpf cyclopamine group, by contrast, none of the animals had a full GCL. Anterior/nasal is left and dorsal is up in all panels. Open arrowheads mark the optic disc/optic nerve head in all panels. A–E are z-projections of confocal stacks taken through the depth of the GCL. Scale bar: 25 μ m. cycl., cyclopamine; veh., vehicle.



Keeping the time: possible cell-intrinsic mechanisms

Our results naturally raise the question of how retinoblasts manage to translate extracellular signals into timing information that will be used hours later. One possibility is that Shh and/or other time-specifying signals might regulate cyclin-dependent kinase inhibitors (CDKIs). In several types of neural progenitor cells, including retinoblasts, gradual accumulation of CDKIs, particularly those of the Kip family, appears to be a mechanism for measuring proliferative time (reviewed by Durand and Raff, 2000; Edlund and Jessell, 1999; Ohnuma and Harris, 2003). Signaling pathways could therefore modulate the subsequent timing of neurogenesis by influencing the initial levels or activities of CDKIs. There is ample evidence for genetic interactions between basic helix-loop-helix proteins (including *Ath5*) and Kip CDKIs (Farah et al., 2000; Kitzmann and Fernandez, 2001; Ohnuma et al., 2002; Vernon et al., 2003). Thus, CDKIs could provide the link between early timing specification signals and subsequent *ath5* expression. Although the ability of Hh to influence CDKI expression is yet untested, PKA activity can influence expression of the Kip gene *p27* in the zebrafish retina (Masai et al., 2005). As Hh derived from the ventral diencephalic midline can act over long distances to regulate other cell cycle genes (Ishibashi and McMahon, 2002), it is plausible that midline Hh signaling might influence retinal CDKI expression. It will be interesting to see whether this mechanism influences the timing of neurogenesis in the retina.

Integration of intrinsic and extrinsic factors during retinal neurogenesis

To date, there have been few attempts to determine how specific neuroblast populations integrate cell-intrinsic and cell-extrinsic information for neurogenic activation. For oligodendrocyte precursors, it has been shown that an intrinsic timer operates, which is licensed by permissive extrinsic signals (Durand and Raff, 2000). Retinoblasts may use a similar cell-intrinsic mechanism to decide when to differentiate (Cayouette et al., 2003). While this work in cell culture, together with our experiments in vivo, highlights the importance of cell-intrinsic factors, RGC neurogenesis is certainly not completely cell-autonomous. First, as in oligodendrocyte precursors, there may be licensing signals – the fact that the majority of transplanted retinoblasts fail to differentiate in our experiments implies the existence of such signals. Second, cell-cell signals may affect steps of RGC differentiation downstream of the cell-intrinsic trigger that activates the neurogenic program (and thus presumably downstream of *ath5* expression).

Third, cell-cell signaling may be necessary to counteract the effects of the intrinsic timer. Our results reveal the existence of an intrinsic tendency toward neurogenesis, but there must be some signal that opposes this tendency – otherwise no retinoblasts would be reserved to make later-born cell types. Similarly, to ensure that the correct number of progenitors become RGCs, there may also be signals that promote neurogenesis over and above the basal level provided by the intrinsic timer. There is strong evidence that Notch, perhaps in concert with other signals, plays both these roles, acting in one context to promote cell cycle exit during the RGC wave (Ohnuma et al., 2002), and in another context to terminate

RGC genesis behind the wave front (Silva et al., 2003). However, Notch probably accomplishes both these roles without affecting the spatiotemporal pattern of differentiation (Ohnuma et al., 2002; Scheer et al., 2001; Silva et al., 2003). Thus, it appears that extrinsic signals balance but do not fundamentally alter the intrinsic program underlying RGC genesis.

Conserved and divergent mechanisms of retinal neurogenesis in insects and vertebrates

In the developing *Drosophila* retina, a progressive cell-cell signaling loop, centered on the *ato* and *hh* genes, initiates neurogenesis (Kumar, 2001). The discovery that close homologs of these genes, *ath5* and *shh*, play a role in differentiation of the first-born neurons of the vertebrate retina led to the hypothesis that the mechanisms for initiating retinal neurogenesis are conserved between flies and vertebrates (reviewed by Kumar, 2001). Despite the appeal of this hypothesis, there have been few attempts to test whether neurogenesis spreads across the vertebrate retina by a fly-like sequential mechanism. In one such study, the peripheral portion of a chick retinal explant, dissected away from the RGC wave front and cultured separately, was still competent to generate RGCs, implying that differentiation does not require a progressive, wave-like mechanism (McCabe et al., 1999). However, a similar experiment in zebrafish yielded the opposite result (Masai et al., 2000). Although there are experimental design differences that might explain the differing results of these two studies, neither has settled the question of whether sequential induction triggers retinal neurogenesis in vertebrates. Here we have devised in-vivo tests of the fly-inspired sequential-induction model, and we have found very little evidence to support it. Our findings indicate that while *hh* and *ato* family genes may have a broadly conserved function in RGC genesis, the cellular context in which they operate differs significantly between vertebrates and insects.

We thank James K. Chen (Stanford) for providing cyclopamine and Judith Eisen (Oregon) and Ichiro Masai (RIKEN) for providing plasmids and fish strains. We also thank E. Ober, C. J. Neumann, and J. K. Chen for helpful comments. The work was supported by an NSF predoctoral fellowship (J.N.K.), by the NIH (EY13855 to H.B. and EY014167 to B.L.) and by a David and Lucille Packard Fellowship (H.B.).

Supplementary material

Supplementary material for this article is available at <http://dev.biologists.org/cgi/content/full/132/11/2573/DC1>

References

- Amato, M. A., Boy, S. and Perron, M. (2004). Hedgehog signaling in vertebrate eye development: a growing puzzle. *Cell. Mol. Life Sci.* **61**, 899–910.
- Brown, N. L., Patel, S., Brzezinski, J. and Glaser, T. (2001). Math5 is required for retinal ganglion cell and optic nerve formation. *Development* **128**, 2497–2508.
- Cayouette, M., Barres, B. A. and Raff, M. (2003). Importance of intrinsic mechanisms in cell fate decisions in the developing rat retina. *Neuron* **40**, 897–904.
- Chen, J. K., Taipale, J., Cooper, M. K. and Beachy, P. A. (2002). Inhibition of Hedgehog signaling by direct binding of cyclopamine to Smoothened. *Genes Dev.* **16**, 2743–2748.

- Chenn, A. and Walsh, C. A. (2002). Regulation of cerebral cortical size by control of cell cycle exit in neural precursors. *Science* **297**, 365-369.
- Dakubo, G. D., Wang, Y. P., Mazerolle, C., Campsall, K., McMahon, A. P. and Wallace, V. A. (2003). Retinal ganglion cell-derived sonic hedgehog signaling is required for optic disc and stalk neuroepithelial cell development. *Development* **130**, 2967-2980.
- Durand, B. and Raff, M. (2000). A cell-intrinsic timer that operates during oligodendrocyte development. *BioEssays* **22**, 64-71.
- Edlund, T. and Jessell, T. M. (1999). Progression from extrinsic to intrinsic signaling in cell fate specification: a view from the nervous system. *Cell* **96**, 211-224.
- Ekker, S. C., Ungar, A. R., Greenstein, P., von Kessler, D. P., Porter, J. A., Moon, R. T. and Beachy, P. A. (1995). Patterning activities of vertebrate hedgehog proteins in the developing eye and brain. *Curr. Biol.* **5**, 944-955.
- Farah, M. H., Olson, J. M., Sucic, H. B., Hume, R. I., Tapscott, S. J. and Turner, D. L. (2000). Generation of neurons by transient expression of neural bHLH proteins in mammalian cells. *Development* **127**, 693-702.
- Ho, R. K. and Kane, D. A. (1990). Cell-autonomous action of zebrafish *spt-1* mutation in specific mesodermal precursors. *Nature* **348**, 728-730.
- Hsiung, F. and Moses, K. (2002). Retinal development in *Drosophila*: specifying the first neuron. *Hum. Mol. Genet.* **11**, 1207-1214.
- Hu, M. and Easter, S. S. (1999). Retinal neurogenesis: the formation of the initial central patch of postmitotic cells. *Dev. Biol.* **207**, 309-321.
- Ishibashi, M. and McMahon, A. P. (2002). A sonic hedgehog-dependent signaling relay regulates growth of diencephalic and mesencephalic primordia in the early mouse embryo. *Development* **129**, 4807-4819.
- Jarman, A. P. (2000). Developmental genetics: vertebrates and insects see eye to eye. *Curr. Biol.* **10**, R857-R859.
- Jarman, A. P., Sun, Y., Jan, L. Y. and Jan, Y. N. (1995). Role of the proneural gene, *atonal*, in formation of *Drosophila* chordotonal organs and photoreceptors. *Development* **121**, 2019-2030.
- Kay, J. N., Finger-Baier, K. C., Roeser, T., Staub, W. and Baier, H. (2001). Retinal ganglion cell genesis requires *lakritz*, a zebrafish *atonal* homolog. *Neuron* **30**, 725-736.
- Kay, J. N., Roeser, T., Mumm, J. S., Godinho, L., Mrejeru, A., Wong, R. O. and Baier, H. (2004). Transient requirement for ganglion cells during assembly of retinal synaptic layers. *Development* **131**, 1331-1342.
- Kitzmann, M. and Fernandez, A. (2001). Crosstalk between cell cycle regulators and the myogenic factor MyoD in skeletal myoblasts. *Cell. Mol. Life Sci.* **58**, 571-579.
- Kumar, J. P. (2001). Signalling pathways in *Drosophila* and vertebrate retinal development. *Nat. Rev. Genet.* **2**, 846-857.
- Li, Z., Hu, M., Ochocinska, M. J., Joseph, N. M. and Easter, S. S., Jr (2000). Modulation of cell proliferation in the embryonic retina of zebrafish (*Danio rerio*). *Dev. Dyn.* **219**, 391-401.
- Livesey, F. J. and Cepko, C. L. (2001). Vertebrate neural cell-fate determination: lessons from the retina. *Nat. Rev. Neurosci.* **2**, 109-118.
- Malicki, J. (2004). Cell fate decisions and patterning in the vertebrate retina: the importance of timing, asymmetry, polarity and waves. *Curr. Opin. Neurobiol.* **14**, 15-21.
- Martinez-Morales, J. R., Del Bene, F., Nica, G., Hammerschmidt, M., Bovolenta, P. and Wittbrodt, J. (2005). Differentiation of the vertebrate retina is coordinated by an FGF signaling center. *Dev. Cell* **8**, 565-574.
- Masai, I., Stemple, D. L., Okamoto, H. and Wilson, S. W. (2000). Midline signals regulate retinal neurogenesis in zebrafish. *Neuron* **27**, 251-263.
- Masai, I., Lele, Z., Yamaguchi, M., Komori, A., Nakata, A., Nishiwaki, Y., Wada, H., Tanaka, H., Nojima, Y., Hammerschmidt, M. et al. (2003). N-cadherin mediates retinal lamination, maintenance of forebrain compartments and patterning of retinal neurites. *Development* **130**, 2479-2494.
- Masai, I., Yamaguchi, M., Tonou-Fujimori, N., Komori, A. and Okamoto, H. (2005). The hedgehog-PKA pathway regulates two distinct steps of the differentiation of retinal ganglion cells: the cell-cycle exit of retinoblasts and their neuronal maturation. *Development* **132**, 1539-1553.
- McCabe, K. L., Gunther, E. C. and Reh, T. A. (1999). The development of the pattern of retinal ganglion cells in the chick retina: mechanisms that control differentiation. *Development* **126**, 5713-5724.
- McLaughlin, T., Hindges, R. and O'Leary, D. D. (2003). Regulation of axial patterning of the retina and its topographic mapping in the brain. *Curr. Opin. Neurobiol.* **13**, 57-69.
- Neumann, C. J. (2001). Pattern formation in the zebrafish retina. *Semin. Cell Dev. Biol.* **12**, 485-490.
- Neumann, C. J. and Nüsslein-Volhard, C. (2000). Patterning of the zebrafish retina by a wave of sonic hedgehog activity. *Science* **289**, 2137-2139.
- Ohnuma, S. and Harris, W. A. (2003). Neurogenesis and the cell cycle. *Neuron* **40**, 199-208.
- Ohnuma, S., Hopper, S., Wang, K. C., Philpott, A. and Harris, W. A. (2002). Co-ordinating retinal histogenesis: early cell cycle exit enhances early cell fate determination in the *Xenopus* retina. *Development* **129**, 2435-2446.
- Pauls, S., Geldmacher-Voss, B. and Campos-Ortega, J. A. (2001). A zebrafish histone variant H2A.F/Z and a transgenic H2A.F/Z:GFP fusion protein for in vivo studies of embryonic development. *Dev. Genes Evol.* **211**, 603-610.
- Perron, M. and Harris, W. A. (2000). Determination of vertebrate retinal progenitor cell fate by the Notch pathway and basic helix-loop-helix transcription factors. *Cell. Mol. Life Sci.* **57**, 215-223.
- Perron, M., Boy, S., Amato, M. A., Viczian, A., Koebnick, K., Pieler, T. and Harris, W. A. (2003). A novel function for Hedgehog signalling in retinal pigment epithelium differentiation. *Development* **130**, 1565-1577.
- Roeser, T. and Baier, H. (2003). Visuomotor behaviors in larval zebrafish after GFP-guided laser ablation of the optic tectum. *J. Neurosci.* **23**, 3726-3734.
- Schauerte, H. E., van Eeden, F. J., Fricke, C., Odenthal, J., Strahle, U. and Haefliger, P. (1998). Sonic hedgehog is not required for the induction of medial floor plate cells in the zebrafish. *Development* **125**, 2983-2993.
- Scheer, N., Groth, A., Hans, S. and Campos-Ortega, J. A. (2001). An instructive function for Notch in promoting gliogenesis in the zebrafish retina. *Development* **128**, 1099-1107.
- Shkumatava, A., Fischer, S., Muller, F., Strahle, U. and Neumann, C. J. (2004). Sonic hedgehog, secreted by amacrine cells, acts as a short-range signal to direct differentiation and lamination in the zebrafish retina. *Development* **131**, 3849-3858.
- Silva, A. O., Ercole, C. E. and McLoon, S. C. (2003). Regulation of ganglion cell production by Notch signaling during retinal development. *J. Neurobiol.* **54**, 511-524.
- Stenkamp, D. L. and Frey, R. A. (2003). Extraretinal and retinal hedgehog signaling sequentially regulate retinal differentiation in zebrafish. *Dev. Biol.* **258**, 349-363.
- Stenkamp, D. L., Frey, R. A., Prabhudesai, S. N. and Raymond, P. A. (2000). Function for Hedgehog genes in zebrafish retinal development. *Dev. Biol.* **220**, 238-252.
- Trevarrow, B., Marks, D. L. and Kimmel, C. B. (1990). Organization of hindbrain segments in the zebrafish embryo. *Neuron* **4**, 669-679.
- Varga, Z. M., Wegner, J. and Westerfield, M. (1999). Anterior movement of ventral diencephalic precursors separates the primordial eye field in the neural plate and requires cyclops. *Development* **126**, 5533-5546.
- Vernon, A. E., Devine, C. and Philpott, A. (2003). The cdk inhibitor p27Xic1 is required for differentiation of primary neurones in *Xenopus*. *Development* **130**, 85-92.
- Vetter, M. L. and Brown, N. L. (2001). The role of basic helix-loop-helix genes in vertebrate retinogenesis. *Semin. Cell Dev. Biol.* **12**, 491-498.
- Wang, S. W., Kim, B. S., Ding, K., Wang, H., Sun, D., Johnson, R. L., Klein, W. H. and Gan, L. (2001). Requirement for *math5* in the development of retinal ganglion cells. *Genes Dev.* **15**, 24-29.
- Wolff, C., Roy, S. and Ingham, P. W. (2003). Multiple muscle cell identities induced by distinct levels and timing of hedgehog activity in the zebrafish embryo. *Curr. Biol.* **13**, 1169-1181.
- Xiao, T., Roeser, T., Staub, W. and Baier, H. (2005). A GFP-based genetic screen reveals mutations disrupting the architecture of the zebrafish retinotectal projection. *Development* (in press).
- Yang, Z., Ding, K., Pan, L., Deng, M. and Gan, L. (2003). *Math5* determines the competence state of retinal ganglion cell progenitors. *Dev. Biol.* **264**, 240-254.
- Zechner, D., Fujita, Y., Hulsken, J., Muller, T., Walther, I., Taketo, M. M., Crenshaw, E. B., 3rd, Birchmeier, W. and Birchmeier, C. (2003). beta-Catenin signals regulate cell growth and the balance between progenitor cell expansion and differentiation in the nervous system. *Dev. Biol.* **258**, 406-418.
- Zhang, X. M. and Yang, X. J. (2001). Regulation of retinal ganglion cell production by Sonic hedgehog. *Development* **128**, 943-957.